$^{56}Fe(n,\alpha)^{53}Cr$ and $^{60}Ni(n,\alpha)^{57}Fe$ reactions at $E_n = 14.1$ MeV

R. Fischer, G. Traxler, M. Uhl, and H. Vonach
Institut für Radiumforschung und Kernphysik, 1090 Wien, Austria
(Received 9 March 1984)

The energy and angular distribution of the α particles from the $^{56}Fe(n,\alpha)$ and $^{60}Ni(n,\alpha)$ reactions for 14.1 MeV incident neutron energy were measured by means of a multitelescope system. The results concerning the total He-production cross sections and the angle-integrated α-emission cross sections $d\sigma/dE_\alpha$ are in fair agreement with previous measurements; for the angular distribution no detailed measurements have as yet been reported. The results are analyzed in the framework of the statistical model of nuclear reactions. Comparison of such calculations with the measured α-emission cross sections allows one to extract nuclear level densities for ^{53}Cr and ^{57}Fe, the residual nuclei reached in the studied reactions in the energy region up to the neutron binding energy, and for ^{56}Fe and ^{60}Ni, the residual nuclei reached by neutron emission for energies around 11 MeV. Within experimental error a purely exponential increase of the level density with excitation energy was found for both ^{53}Cr and ^{57}Fe. The spin cutoff parameters for ^{53}Cr and ^{57}Fe derived from the data indicate that there is no reduction of the effective moment of inertia below the rigid body value.

I. INTRODUCTION

The study of (n,α) reactions induced by 14 MeV neutrons in medium-weight nuclei offers favorable conditions for the determination of the level densities of both the residual nuclei reached by the α particle and by neutron emission from the investigated compound nucleus.[1] As reliable level density values—except at the neutron binding energy—are still rather scarce,[1] the reactions $^{56}Fe(n,\alpha)^{53}Cr$ and $^{60}Ni(n,\alpha)^{57}Fe$ were investigated in order to derive level density values for the corresponding residual nuclei ^{53}Cr, ^{56}Fe, ^{57}Fe, and ^{60}Ni.

In addition, the study of these reactions is also important for applied purposes as both iron and nickel are important structural materials for future fusion reactors. There has been one previous measurement of both reactions;[2] however, a second independent measurement is highly desirable for important nuclear data. In addition, the mentioned study[2] was done primarily for applied purposes and thus the high energy part of the α spectra was not measured as accurately as needed for optimum determination of nuclear level densities and no detailed measurements of the angular distributions had been done.

In Sec. II we report on the experimental procedures and the methods of data analysis used to derive the absolute double differential α-emission cross sections. In Sec. III we report the experimental results and compare them in detail to those of Ref. 2, and in Sec. IV the statistical model analysis and the derivation of level density values is described in detail.

II. EXPERIMENT AND DATA ANALYSIS

The (n,α) reactions were studied by means of a multitelescope system irradiated by 14.1 MeV neutrons produced in the 250 keV accelerator of the Institut für Radiumforschung und Kernphysik. As both the multitelescope system[3] and the procedures used for the analysis of the data and their transformation into double-differential particle emission spectra have been described before,[4] only a few details specific to this experiment are given in the following.

Targets of iron and nickel metal enriched to more than 99% in ^{56}Fe and ^{60}Ni, respectively, were used. The rolled targets had an average thickness of 2.15 ± 2 % (^{56}Fe) and 2.34 ± 2 % mg/cm^2 (^{60}Ni), as determined both by weighing and by measuring the α-energy loss. The homogeneity of the targets was investigated by α-energy loss measurements at nine positions within each target. From these measurements it is estimated that the effective target thickness for each individual telescope does not deviate by more than 3.5% from the average. In order to further reduce the effect of these inhomogeneities the target was rotated by 180° in the middle of each experiment. In this way any influence of the target inhomogeneities on the forward-backward cross section ratio was eliminated and also the effects of possible small asymmetries between the two halves of the multiwire counter. No difference between the two measurements was found within the statistical error of the data. The results were corrected in the usual way for the energy loss in the targets, that is, all particles were assumed to have lost an energy corresponding to half the target thickness. Each of the above targets was irradiated for about 200 h at a neutron source strength of 8.3×10^9 n/sec resulting in neutron fluxes from 4.5×10^5 n/cm^2 sec to 2.0×10^5 n/cm^2 sec.

III. RESULTS

As the primary result of the data analysis described in Sec. II, double-differential α-emission spectra were obtained for 16 reaction angles ranging from 22°—165°; the angular resolution of each telescope was on average 13°.[3] Because of the limited statistics of the experiments (total number of true events for either reaction $\sim2.10^4$), the individual spectra have rather large statistical errors.

TABLE I. Angle-integrated α-particle emission cross sections for the ^{56}Fe(n,$x\alpha$) and ^{60}Ni(n,$x\alpha$) reactions at E_n=14.1 MeV.

E_α (channel energy) (MeV)	$\frac{d\sigma}{dE_\alpha}$ (^{56}Fe + n) (mb/MeV)	$\frac{d\sigma}{dE_\alpha}$ (^{60}Ni + n) (mb/MeV)
5–6	1.69±0.20[a]	2.98±0.25[a]
6–7	4.39±0.28	5.59±0.34
7–8	8.60±0.43	10.91±0.55
8–9	10.63±0.51	15.23±0.73
9–10	7.45±0.37	13.54±0.65
10–11	4.63±0.25	8.96±0.44
11–12	2.98±0.18	4.87±0.26
12–13	2.06±0.13	3.35±0.19
13–14	0.75±0.08	1.46±0.11
14–15	0.23±0.06	1.04±0.09
15–16		0.28±0.06

[a]The fully correlated part of the errors amounts to 4.4% of the cross-section values.

Therefore more meaningful data were obtained by integrating the results over either energy or angle. Thus we will in the following present and discuss the angle-integrated α spectrum, the α-particle angular distributions for a few rather large α-energy regions, and the total α-emission cross sections.

Table I gives the results for the angle-integrated α-emission cross sections for 1 MeV energy bins which correspond roughly to the energy resolution of the experiments. The errors given are effective 1σ errors obtained by adding the statistical errors and estimates of all identified sources of systematic error in quadrature. Systematic errors are included for uncertainties in neutron flux (3%), effective target thickness (3.5%), solid angle of telescopes (1.7%), dead time correction (1%), and the uncertainties

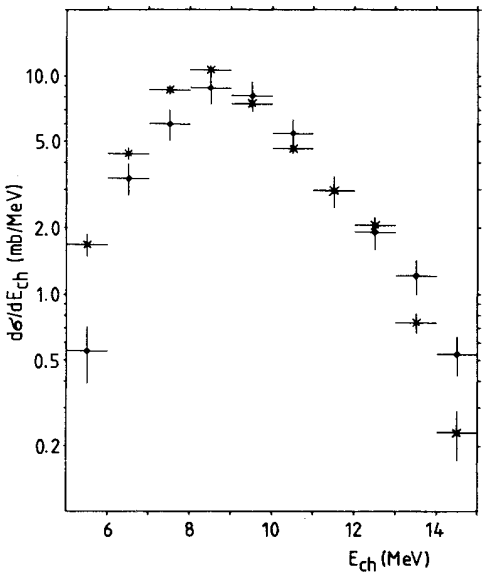

FIG. 1. The angle-integrated α-emission cross section for the ^{56}Fe(n,α) reaction. × denotes the present results (E_n=14.1 MeV) and ● denotes the results of Refs. 2 (E_n=15 MeV).

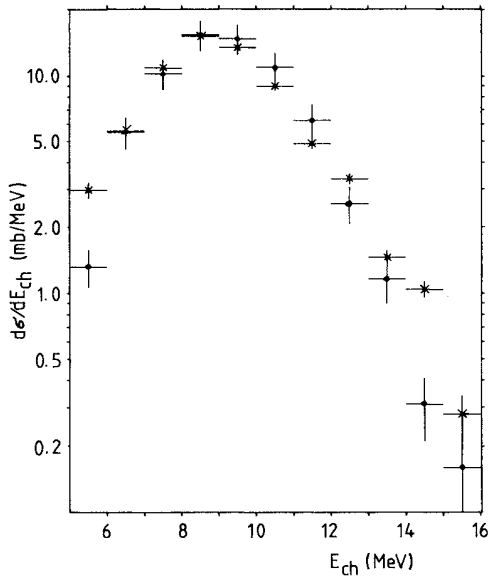

FIG. 2. The angle integrated α-emission cross section for the ^{60}Ni(n,α) reaction. × denotes the present results (E_n=14.1 MeV) and ● denotes the results of Ref. 2 (E_n=15 MeV).

in the chosen boundaries for particle identification (2%). The energy calibration of the CsI crystal[3,4] is believed to be accurate to 0.3 MeV. In Figs. 1 and 2 these results are compared with the measurements reported in Ref. 2, which for this purpose were transformed into the c.m. system. The authors gratefully acknowledge the cooperation of Dr. R. C. Haight who supplied the numerical data needed for this transformation. There is good overall agreement between the two measurements, but in detail there exist two areas of discrepancy.

(1) At low α energy ($E_{\alpha ch}$ < 6 MeV) the α-emission cross section of Ref. 2 is much smaller than ours, which cannot be explained by the slightly different incident neutron energies. In this energy range our measurements are complicated by a rather large background (effect to background ratio 1.5:1) and the Livermore data indicate experimental problems as there are considerable discrepancies between the emission cross sections for the different angles.

(2) Considering the difference in incident energies the high energy parts of the α spectra for the ^{60}Ni(n,α) reaction definitely disagree beyond the experimental errors. No obvious reason for this discrepancy could be found. The total α-emission cross sections obtained by numerical integration of the $d\sigma/dE_\alpha$ values are given in Table II.

TABLE II. Total α-emission cross sections in the ^{56}Fe(n,$x\alpha$) and ^{60}Ni(n,$x\alpha$) reactions.

E_n (MeV)	σ [^{56}Fe(n,$x\alpha$)] (mb)	σ [^{60}Ni(n,$x\alpha$)] (mb)	Ref.
14.1	44±2.	69.6±3.1	This work
15	41±7.	76 ±12	2
15	48±3.	79 ±6	5

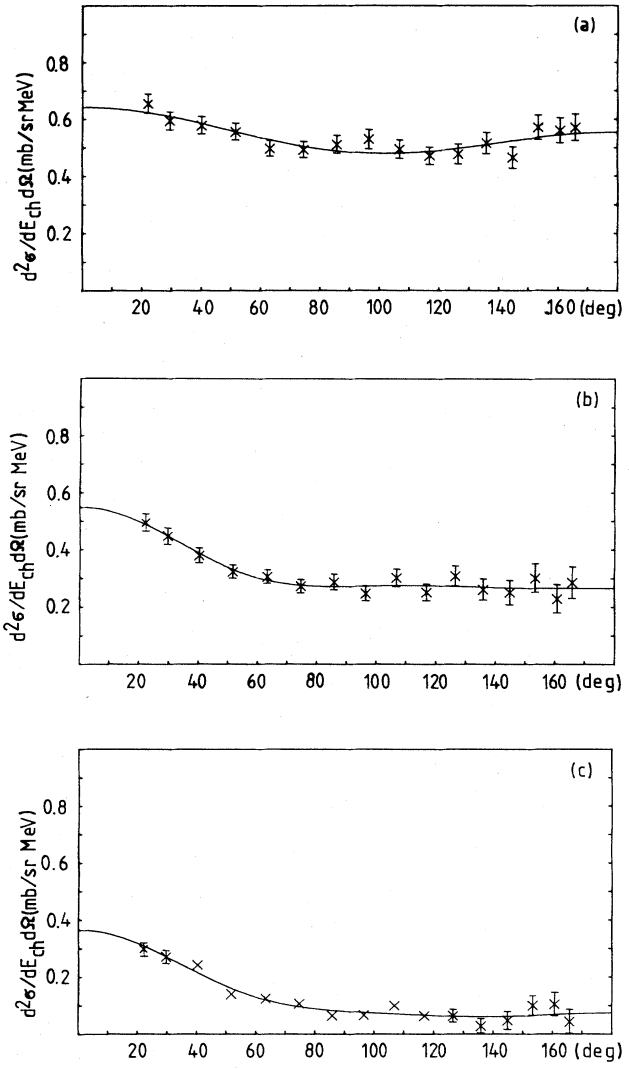

FIG. 3. Angular distributions for different α-energy bins for the ^{56}Fe(n,α) reaction: (a) $E_{\alpha ch}=6-10$ MeV, (b) $E_{\alpha ch}=10-12$ MeV; and (c) $E_{\alpha ch}=12-14$ MeV. The solid curves denote the Legendre fits to data.

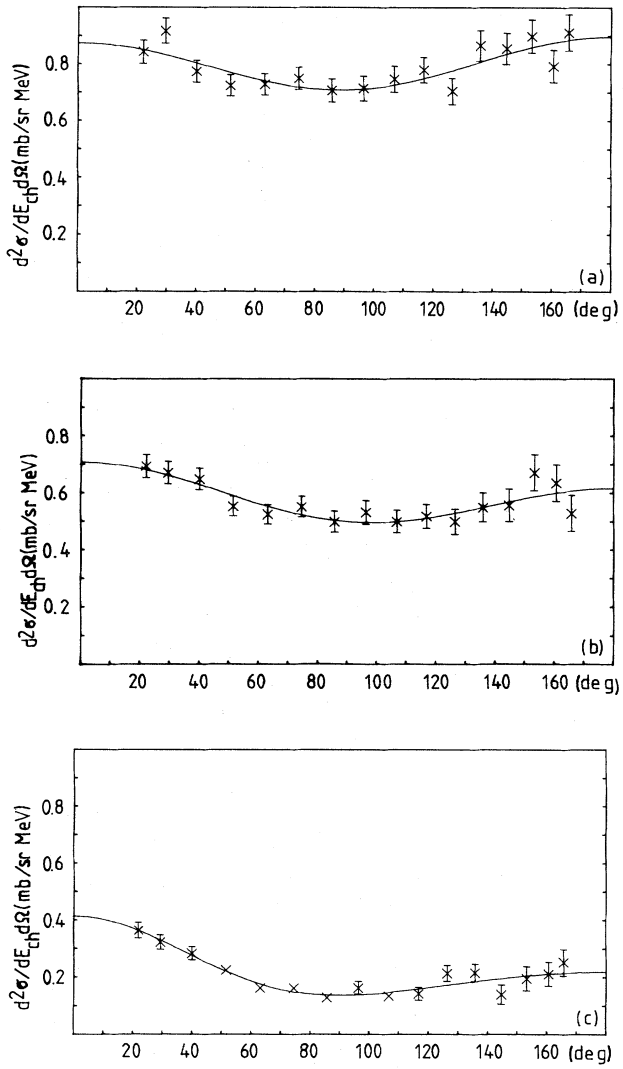

FIG. 4. Angular distributions for different α-energy bins for the ^{60}Ni(n,α) reaction: (a) $E_{\alpha ch}=6-10$ MeV, (b) $E_{\alpha ch}=10-12$ MeV, and (c) $E_{\alpha ch}=12-14$ MeV. The solid curves denote the Legendre fits to data.

As the table shows they agree within experimental error both with the results of Ref. 2 and the results of helium accumulation measurements;[5] in this comparison it has to be considered that at the higher incident neutron energies of Refs. 2 and 5 the α-emission cross section should be about 5–10 % higher than at our energy of 14.1 MeV.

Figures 3 and 4 show the angular distributions obtained for different α-energy regions. In these figures the data points are given with their uncorrelated errors only. The figures show that there are considerable contributions from noncompound reactions at the highest α-particle energies probably due to direct excitations populating low lying levels as already found in the study of the ^{50}Cr(n,α) reaction.[4] In the region of the evaporation peak [see Figs. 3(a) and 4(a)] the angular distributions are approximately symmetrical around 90° and show a small minimum at 90° as expected according to the Hauser-Feshbach (HF) theory. The size of this minimum is about the same as in our ^{50}Cr(n,α) measurement (Ref. 4) and much smaller than claimed in some of the early work on (n,α) reactions,[6,7] which probably suffered from some unidentified systematic errors. The implication of this for the effective nuclear moment of inertia will be discussed in Sec. IV.

IV. DETERMINATION OF NUCLEAR LEVEL DENSITIES AND SPIN CUTOFF FACTORS FROM A STATISTICAL MODEL ANALYSIS OF THE RESULTS OF SEC. III

Measurements of evaporation spectra have so far mostly been analyzed in two ways:

(1) The nuclear level density of the residual nucleus populated in the studied reactions was calculated from the

measured spectrum by means of the so-called Weisskopf-Ewing approximation neglecting angular momentum effects.

(2) The measured spectra are compared to the results of Hauser-Feshbach calculations with correct treatment of spin and parity conservation and the level density parameters of the residual nuclei needed for this purpose are varied until reasonable agreement with the measured spectra is obtained.

Both methods have serious disadvantages. Method one easily allows extraction of level density values; however, neglect of angular momentum effects definitely introduces considerable errors for reactions involving α particles.[8] On the other hand, method two does not easily allow the extraction of level density values and estimates of their uncertainties quantitatively.

For this reason, in the following analysis a third procedure avoiding the mentioned shortcomings of both methods is used. Essentially, the method of extraction of level density values by means of the Weisskopf approximation is generalized to the case of statistical model calculations using the full Hauser-Feshbach formalism. This procedure is discussed in detail in Ref. 1. Thus, in the following we will only give a very short description of the various steps involved in this analysis.

The extraction of the total level densities summed over all spin and parity values was done in the following way:

(1) The angle integrated α-particle emission cross sections were calculated within the Hauser-Feshbach formalism using the code STAPRE (Ref. 9) using a set of parameters (transmission coefficients and level density parameters) which had previously been derived in an overall evaluation of neutron cross sections for structural materials.[10]

(2) The results of this calculation are compared to the α-emission cross section measurements in the region of resolved levels. In this region, the cross sections are essentially determined by the ratio of the decay widths to these levels to the total decay width of the compound nuclei, which is dominated by the neutron width and thus by the level density of the nuclei reached by neutron emission in the excitation energy range populated in the evaporation process. Therefore, the level density parameters of this residual nucleus are slightly varied until agreement with the measured α-emission cross section in the region of resolved levels is obtained. Actually the level density of the residual nuclei reached by proton emission were also adjusted in such a way that the proton emission cross sections remained constant at the values derived in the evaluation of Strohmaier and Uhl.[10] This procedure is not unique; for example, in the framework of the back-shifted Fermi-gas model a fit can be obtained with different combinations of the parameters a and Δ. However, as shown in Ref. 1, the level densities calculated with these different parameter combinations coincide to good approximation at an excitation energy of $E^*=E_0-2T$, E_0 being the incident neutron energy and T the nuclear temperature at E_0; for the reactions studied in this work this means that the described procedure allows us to derive level density values for ^{56}Fe and ^{60}Ni at $U\sim 11$ MeV.

(3) Having fixed the level densities of the residual nuclei reached by neutron and proton emission in the described way, we repeat the calculation of the α-emission cross sections and get the level densities for the residual nuclei reached by α emission by means of the relation

$$\rho(U)=\rho(U)_{\text{assumed}}\left[\frac{\left[\frac{d\sigma}{d\epsilon_\alpha}\right]_{\text{meas}}}{\left[\frac{d\sigma}{d\epsilon_\alpha}\right]_{\text{calc}}}\right]_{\epsilon_\alpha=\epsilon_{\alpha\max}-U}, \qquad (1)$$

where $\rho(U)$ is the total level density of the residual nucleus according to the α-emission cross section $(d\sigma/d\epsilon_\alpha)_{\text{meas}}$ and $\rho(U)_{\text{assumed}}$ is the total level density of the residual nucleus assumed in the calculation of $(d\sigma/d\epsilon_\alpha)_{\text{calc}}$; ϵ_α is the channel energy for α-particle emission.

The above analysis assumes that the reaction proceeds completely via compound nucleus formation and decay. As is obvious from the measured angular distribution, there are, however, noticeable noncompound contributions at the highest α energies. In order to minimize their effects in the analysis two steps were taken:

(1) The analysis was done only for the α-emission spectrum integrated over the backward hemisphere.

(2) Comparison with the calculations for population of resolved levels was not done for the ground state and the lowest excited levels but for the levels in the excitation energy range $U=2.1$–3.1 MeV for ^{53}Cr and 1.22–2.22 MeV for ^{57}Fe, which is about the limit up to which all levels of these nuclei are reliably known. In this way the highest energy part of the α spectra, which is especially contaminated with noncompound particles, is not needed for the analysis.

For estimating the uncertainties of the level densities derived by step two by use of Eq. (1), we have to consider both the uncertainties of the measured $d\sigma/d\epsilon_\alpha$ values and the uncertainties of the calculated α-emission cross sections due to the uncertainties of the parameters entering into the calculations, respectively. The most important parameters are the following: transmission coefficients, for the incoming and all outgoing particles; assumed spin dependence for level densities of all residual nuclei and the uncertainty of the compound nucleus formation cross sections due to the uncertainty of the direct and precompound fractions (see Sec. 3.2.5 of Ref. 1). In addition, an estimate of possible noncompound contributions at the high energy end of the α spectra used for the derivation of the level densities has to be made and included in the total error estimate.

These uncertainties were estimated in the following way:

(1) Uncertainty in optical model parameters for incoming neutrons, estimated from calculations using different optical model parameter sets [Los Alamos Scientific Laboratory (LASL) potential for ^{56}Fe (Ref. 11) and Perey-Buck global optical model parameters[12]]. Error contribution to level densities of ^{56}Fe and ^{60}Ni amounts to $\sim 5\%$.

(2) Uncertainty in the fractions f_D and f_{pre} for direct and precompound emission reducing the compound nucleus formation cross sections below the optical model absorption cross section by $[1-(f_D+f_{pre})]$. An uncertainty of 30% was assumed for both the f_D and f_{pre} values resulting in an uncertainty of $\sim 8\%$ for $[1-(f_D+f_{pre})]$ and thus for the level densities of ^{56}Fe and ^{60}Ni.

(3) Uncertainty in the optical model parameters for the outgoing neutrons. The effect on the calculated cross sections was again estimated by calculations with the two mentioned potentials resulting in an uncertainty estimate of 15% for the level densities of ^{50}Fe and ^{60}Ni.

(4) Uncertainty of the optical model parameters for the outgoing α particles. An uncertainty of 7% was estimated for the level densities of ^{53}Cr and ^{57}Fe due to this cause considering the accuracy of the total reaction cross section measurements[13] which support the used potential.[14]

(5) Uncertainty in the spin distribution of the nuclear levels: Cross section calculations were done in which the effective nuclear moment of inertia was varied by 30% from the otherwise assumed rigid body value. This results in uncertainty contributions of $\sim 10\%$ for the level densities of ^{56}Fe and ^{60}Ni and $\sim 7\%$ for those of ^{53}Cr and ^{57}Fe.

(6) An uncertainty of 10% was assumed for possible noncompound contributions in the measured α-emission cross section at the high energy end of the used part of the spectrum.

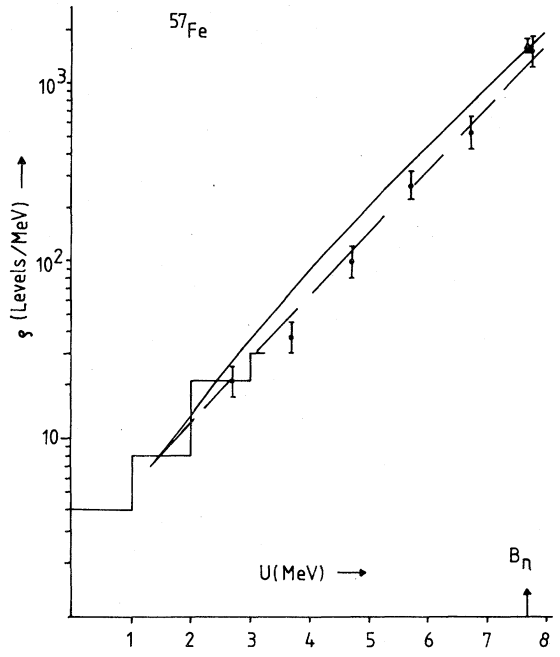

FIG. 6. Level density of ^{57}Fe. The level density is derived from s-wave neutron resonance spacing assuming a rigid body moment of inertia ($\sigma=4.23$); —— denotes the back-shifted Fermi gas with $a=6.4$ MeV^{-1} and $\Delta=-1.09$ MeV. Other symbols are as in Fig. 5.

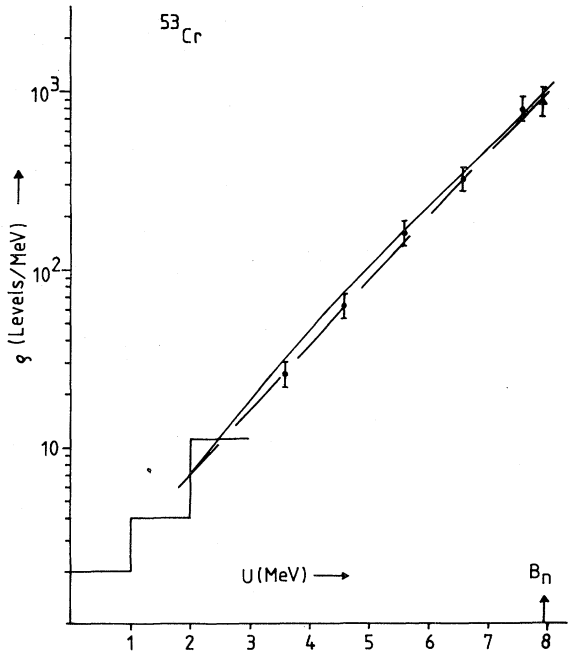

FIG. 5. Level density of ^{53}Cr. The histogram is derived from the counting of resolved levels: ● denotes the level density derived from $d\sigma/dE_\alpha$ values; Δ denotes the level density derived from s-wave neutron resonance spacing, assuming a rigid body moment of inertia ($\sigma=4.04$); —— denotes the back-shifted Fermi gas with $a=5.96$ MeV^{-1} and $\Delta=-0.72$ MeV; and — — — denotes the constant temperature fit to experimental results.

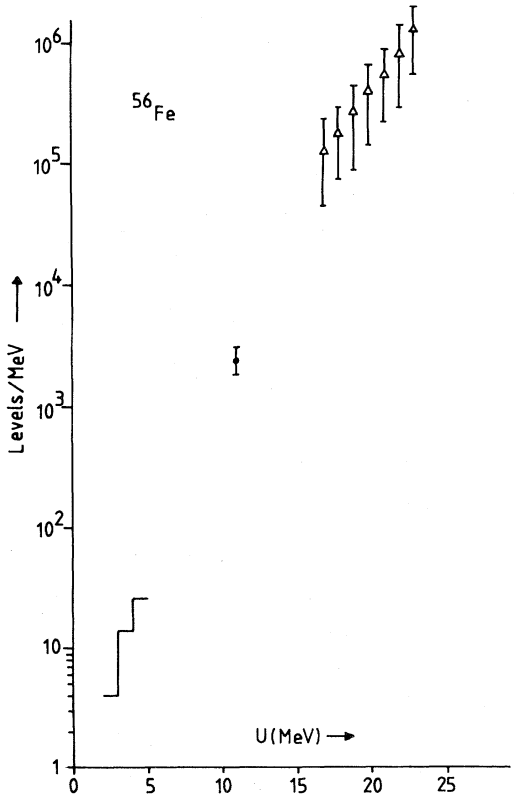

FIG. 7. Level density of ^{56}Fe. The histogram is derived from counting of discrete levels: ● denotes the level density derived from α-emission cross sections into the region of resolved levels, and Δ denotes level densities from Ericson fluctuations (Ref. 16).

TABLE III. Spin cutoff factors of ^{53}Cr and ^{57}Fe.

Nucleus	U (MeV)	σ	Method
^{53}Cr	7.94	4.1±0.6	Comparison with average s-wave spacing
^{53}Cr	3.85—7.85	$4.^{+1.6}_{-0.6}$	Angular distribution of evaporated α particles
^{57}Fe	7.65	3.8±0.4	Comparison with average s-wave spacing
^{57}Fe	4.2—7.7	$3.8^{+1.4}_{-0.5}$	Angular distribution of evaporated α particles

The level densities of ^{53}Cr and ^{57}Fe derived in this way are shown in Figs. 5 and 6 and are compared with the level densities derived from counting of discrete levels and the value derived from the density of s-wave resonances[15] using spin cutoff factors for ^{56}Fe and ^{60}Ni which correspond to a rigid body value for the effective nuclear moment of inertia. In addition, the figures show the prediction of the back-shifted Fermi-gas model with parameters adjusted to the density of discrete levels and the density of neutron resonances.[15]

The measured level density values are in somewhat better agreement with a simple exponential dependence of the level density with excitation energy than with the Fermi-gas form. Also, the accuracy is not quite sufficient to decide on the relatively small difference between the two shapes. Analyzed in terms of a constant temperature model, our measurements give a nuclear temperature of 1.20±0.03 MeV for ^{53}Cr and 1.22±0.03 MeV for ^{57}Fe in the excitation energy region below the neutron binding energy.

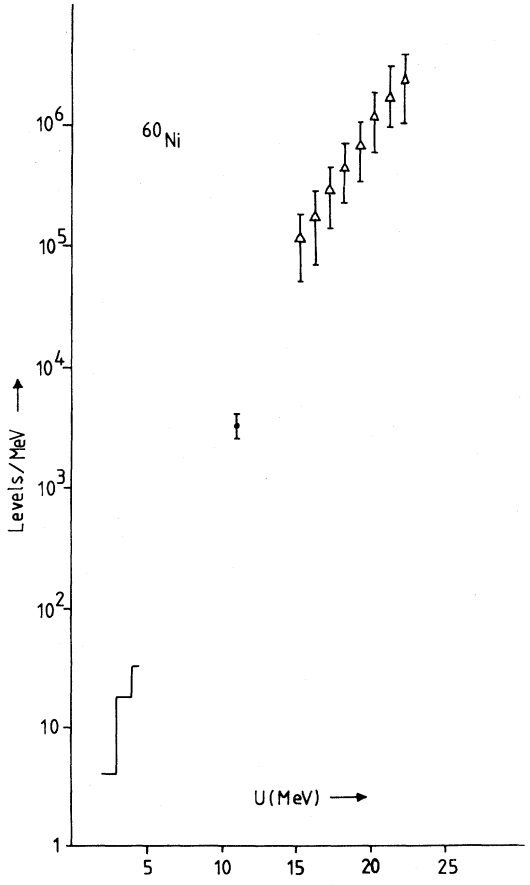

FIG. 8. Level density of ^{60}Ni. Symbols are as in Fig. 7.

Figures 7 and 8 compare the level density values for ^{56}Fe and ^{60}Ni at 11 MeV derived from the α-emission cross sections into the region of discrete levels with the level density values from counting of discrete levels and from Ericson fluctuations.[16] As the figures show, there is reasonable agreement between the level density values derived by the different methods. If the level densities from level counting and our value at U=11 MeV are combined one gets an average nuclear temperature of 1.44±0.07 and 1.42±0.17 for ^{56}Fe and ^{60}Ni in the excitation energy range U=4—11 MeV, which is considerably higher than the values found for ^{53}Cr and ^{57}Fe and suggests the possible existence of an odd-even effect in these temperature values.

Information on the spin cutoff parameter σ can be obtained from the measured data in two ways:

(1) Comparison of the total level density at the neutron binding energy with the average spacing of s-wave neutron resonances as shown in Figs. 5 and 6.

(2) Comparison of the α-particle angular distribution in the region of the evaporation peak with statistical model calculations for different values of the spin cutoff factor σ. The spin cutoff factors determined in this way are shown in Table III. The values for ^{53}Cr correspond almost exactly to an effective nuclear moment of inertia equal to the rigid body value (with r_0=1.25 fm), the ^{57}Fe results imply a reduction of about 10% below this value. These results are in good agreement with other determinations of the spin cutoff factor in this mass range from (α,α'), (α,p), (p,α),[17,18] and (α,n) (Refs. 19 and 20) reactions.

ACKNOWLEDGMENTS

The authors gratefully acknowledge the support of Dr. Maier-Komor who provided the excellent rolled ^{56}Fe and ^{60}Ni targets. This work was supported by Fonds zur Förderung der Wissenschaftlichen Forschung in Österreich.

[1]H. Vonach, Proceedings of the International Atomic Energy Agency Advisory Group Meeting on Basic and Applied Problems of Nuclear Level Densities, Brookhaven National Laboratory Report BNL-NCS-51694, 1983.
[2]S. M. Grimes *et al.*, Phys. Rev. C **19**, 2127 (1979).
[3]C. Derndorfer *et al.*, Nucl. Instrum. Methods **187**, 423 (1981).
[4]C. Derndorfer *et al.*, Z. Phys. A **301**, 327 (1981).
[5]D. W. Kneff *et al.*, Proceedings of the Symposium on Neutron Cross Sections from 10 to 50 MeV, Brookhaven National Laboratory Report BNL-NCS-51245, 1980, p. 289.
[6]W. H. Patzak and H. Vonach, Nucl. Phys. **39**, 263 (1962).
[7]M. Bormann, Habilitationsschrift, Universität Hamburg, 1965.
[8]H. Vonach, Habilitationsschrift, Technische Universität München, 1964.
[9]M. Uhl, International Atomic Energy Agency Report No. 190, 1976, Vol. II, p. 361.
[10]B. Strohmaier and M. Uhl, *Proceedings of the International Conference on Nuclear Data for Science and Technology, Antwerp, 1982* (Reidel, Dordrecht, 1983), p. 552.
[11]E. Arthur and P. G. Young, Los Alamos National Laboratory Report LA-8626 MS (ENDF-304), 1980.
[12]F. G. Perey and B. Buck, Nucl. Phys. **32**, 353 (1962).
[13]H. Vonach, R. C. Haight, and G. Winkler, Phys. Rev. C **28**, 2259 (1983).
[14]L. McFadden and G. R. Satchler, Nucl. Phys. **84**, 177 (1966).
[15]F. H. Fröhner, K. Wisshak, and F. Kaeppeler, Kernforschungszentrum, Karlsruhe Report No. 2899, 1977.
[16]J. R. Huizenga *et al.*, Phys. Rev. **182**, 1149 (1969).
[17]C. C. Lu, L. C. Vaz, and J. R. Huizenga, Nucl. Phys. **A197**, 321 (1972).
[18]H. Vonach and J. R. Huizenga, Phys. Rev. **149**, 844 (1966).
[19]P. Hille *et al.*, Nucl. Phys. **A232**, 157 (1974).
[20]S. M. Grimes *et al.*, Phys. Rev. C **10**, 2273 (1974).